The Metron Model: a Unified Deterministic Theory of Fields and Particles – a Progress Report

Klaus HASSELMANN and Susanne HASSELMANN

Max-Planck-Institute for Meteorology, Bundestrasse 55, 20146 Hamburg, Germany
E-mail: *klaus.hasselmann@dkrz.de*

Metron computations of the double-slit diffraction of a particle beam are in good agreement with quantum theory, demonstrating that wave-particle duality can be explained quantitatively within the framework of a deterministic particle model. Preliminary forward-modelling computations of the structure the electron are consistent with previous metron predictions from inverse modelling, but work on this complex numerical problem is still in progress.

1 Introduction

In a previous four-part paper [6] (see also [7]) the metron concept of a general unified deterministic theory of fields was developed. The present paper reports on recent numerical computations of some of the basic properties of this model.

The metron model is based on the premise that, in contrast to standard quantum field theory, particles exist as real objects. It is hypothesized that they represent non-linear soliton-type solutions of Einstein's gravitational equations in a higher (at least eight) dimensional matter-free space. The *metron* solutions (*metr*ic solit*ons*) are composed of a non-linear core region, which defines the particle properties (mass, charge, spin, weak and strong coupling constants, etc.), and a linear far-field region, which carries the classical gravitational and electromagnetic fields, as well as a high-frequency periodic field that satisfies the de Broglie dispersion relation. The de Broglie field alone, being oscillatory, exerts no mean force. However, mean forces are generated through quadratic interactions of the de Broglie field with its own scattered field, produced by interactions with other matter, thereby producing wave-like interference phenomena.

Apart from dimensional units defining the background metric (such as the velocity of light), the vacuum Einstein equations contain no physical constants. All particle properties and other physical constants must therefore follow from the structure of the particle solutions themselves.

In the particle rest-frame, the metron solutions are assumed to be periodic with respect to time (x^4) and the extra space coordinates $(x^5, \ldots, x^8)$, in accordance with the original Kaluza–Klein method for removing the non-observed dependence of the metric on the extra-space coordinates. The wave-numbers k_4 and $k_5, \ldots, k_8$ define the mass, electroweak and strong coupling constants, respectively.

The bound-state metron solutions are generated through the mutual interaction between oscillatory and mean metric field components. The oscillatory components represent eigenmodes (and forced higher harmonics) which are trapped in the particle core by the mean metric field, which acts as a localized wave-guide. The mean wave-guide field, in turn, is generated by quadratic interactions (radiation stresses or currents) between the trapped eigenmode fields.

In addition to demonstrating that metron solutions exist, the metron model must resolve a number of other fundamental issues. These were addressed in [6] using inverse modelling methods (a more detailed summary is given in [6, Part 1]): Following the demonstration, for a simple scalar analogue of the Einstein equations, that bound-state solutions can indeed be

generated by the wave-mode/wave-guide trapping mechanism [6, Part 1], it was shown that for metron solutions with appropriate polarization structures the metron model is able to

1) recover both the gravitational forces and the electromagnetic forces of charged point-like particles, including spin, in accordance with the classical Einstein–Dirac–Maxwell system of quantum theory [6, Part 2];

2) reproduce qualitatively, through resonant interactions between primary and secondary de Broglie waves, the resonant Bragg scattering of particles at a periodic lattice and the basic structure of discrete atomic spectra [6, Part 3];

3) resolve the EPR paradox, while circumventing the non-existence theorem of Bell for hidden-variable theories (such as the metron model) by invoking the time-reversal symmetry of interactions at the microphysical level, as developed by Wheeler and Feynman [11,12] ([6, Part 3]);

4) explain the symmetries of the Standard Model of Quantum Field Theory in terms of geometrical symmetries of the metron solutions in extra space [6, Part 4].

In the present paper we extend these general results through more detailed numerical computations. First, we show that the metron model is able to reproduce quantitatively the results of the double-slit refraction experiment. We then apply the forward-modelling approach in first steps towards computing the metron solution for the simplest possible particle, the electron (which we have chosen rather than the more enigmatic neutrino, see [6, Part 4]). The paper concludes with an outlook on further work.

2   The double-slit refraction experiment

Few experiments have been more intensively discussed since the conception of quantum theory than the refraction of a particle beam at a double slit. If the beam is sufficiently weak, the position of an individual particle can be located before and after it has passed through the slits. It is readily understandable already from classical physics (through the uncertainties introduced through the measurement process) that the the initial and/or final position of the particle can not be determined with sufficient accuracy to decide through which of the two slits the particle has actually passed. However, the positivistic Copenhagen position, that it is therefore meaningless to state that the particle has passed through one or the other of the slits, represents a radical departure from the classical view that physics can be described by real, existing objects. Physicists have therefore sought alternative explanations of the wave-like interference patterns of the double-slit experiment that are consistent with classical physics.

A well known alternative classical interpretation is the guiding- or pilot-wave model of de Broglie [3–5] and Bohm [2], popularized also by Bell [1]. The basic concept is that the interference patterns are generated through a guiding "pilot wave" that accompanies the particles. However, a basic difficulty of this model is the rather nebulous origin of the pilot wave and its interaction with the particle that it guides. The metron model offers a simple interpretation of the de Broglie–Bohm model: the guiding "pilot wave" is none other than the de Broglie wave component of the metron bound-state solution. Its interaction with the particle that it guides arises through the interaction of the primary de Broglie wave with the scattered or refracted secondary wave that is generated when the primary wave interacts with another object. Following the qualitative application of this concept to Bragg scattering and the structure of discrete atomic spectra in [6, Part 3], we show now that the interaction between the intrinisic primary and refracted secondary de Broglie wave field is able to reproduce quantitatively the detailed refraction pattern of the double-slit experiment.

Consider a homogeneous monochromatic beam of particles travelling in the x-direction that impinges on a screen at $x = 0$ that contains two slits, $a/2 < |y| < a/2 + d$, of width d and separation a centred at $y = 0$. According to quantum theory, the incident beam is described by a state function $\psi_i(x, y) = \exp(ikx)$, where $k = mU/\hbar$, m is the particle mass, U the particle velocity, and we have dropped irrelevant frequency dependent and normalization factors. In the first-order Kirchhoff approximation, the refracted wave function is given, for $y \ll x$, by

$$\psi_r(x, y) = (2d/z) \exp(ikx)[\sin\{(1 + \alpha)z\} - \sin(\alpha z)], \tag{1}$$

where $z = kd\theta$, $\theta = y/x$ and $\alpha = a/2d$.

We compare now quantum theoretical refracted particle flux proportional to $|\psi_r|^2$ with the refracted beam computed using the metron model. An individual particle approaching the screen on a path $x = Ut$, $y = y_0 = $ const (where y_0 lies in one of the slits) carries with it a de Broglie field $\hat{\psi}_i = f_0(x - Ut, y - y_0)\psi_i$, where ψ_i is the same incident field as in the quantum theoretical case, and $f_0(x - Ut, y - y_0)$ is an additional modulation factor describing the decrease of the (primary) metron de Broglie field with distance from the particle core. For the refracted (secondary) de Broglie field we obtain, in analogy to equation (1), the field $\hat{\psi}_r(x, y) = f_r(x - Ut, y - y_0)\psi_r(x, y)$, where $f_r(x - Ut, y - y_0)$ is a further modulation factor describing the decrease of the refracted field with distance from a (hypothetical) reference particle on the non-refracted particle path. The relations for both $\psi_r(x, y)$ and $\hat{\psi}_r(x, y)$ apply in the far-field region behind the slits.

To compute the path of the refracted particle, we need to compute the force exerted on the particle by the non-linear interaction between the primary and secondary de Broglie fields. This is governed by a potential function Φ, which is determined by the product $\hat{\psi}_r\hat{\psi}_p^*$ of the refracted secondary field $\hat{\psi}_r(x, y)$ with the particle's (complex conjugate) primary field $\hat{\psi}_p^*$, integrated over the core region of the particle (see [6, Parts 2 and 3]). The phase relation between the primary and secondary fields (with respect to the periodicity in $z = kd\theta$) depends on the path of the refracted particle relative to its refracted field.

Assume that in passing through the near-field of the slits, the particle is deflected by the near-field interactions into some initial direction θ_0, therefore propagating first along a path $x = Ut$, $y = y_0 + \theta_0 Ut$ before entering into the far-field region. The evolution of the further particle path $y(x)$ in the far-field region is then determined by the path equations

$$\frac{d\theta}{dx} = \frac{v - \theta}{x}, \qquad \frac{dv}{dx} = U\frac{\partial\Phi}{\partial y}, \tag{2}$$

for $\theta = \theta(x)$, $v = v(x)$, where $y = \theta x$, $v = U\,dy/dx$, with initial conditions $\theta(0) = \theta_0$, $v(0) = v_0$. The phase of the refracted secondary de Broglie field relative to the intrinsic primary de Broglie field of the particle depends on the point y_0 at which the particle passes the slit, together with the direction θ of the particle path. If one averages over all positions y_0 in the two slits, one obtains the same phase for the intrinsic de Broglie field as for the refraction amplitudes ψ_r and $\hat{\psi}_r(x, y)$. Taking this average phase value as a first approximation, and noting that the gradient of the potential Φ is dominated by the oscillatory dependence on z, we find that the net force acting on the refracted particle is proportional to $\partial\Phi/\partial y \approx$ const $\partial|\psi_r|^2/\partial y$. For const > 0, the force has the effect of focussing the refracted particles towards the maximal values of $|\psi_r|^2$, i.e. into the regions of maximum refracted particle flux as given by quantum theory.

That this is indeed the case is demonstrated in Fig. 1[1]: the metron computation agrees very closely with the quantum-theoretical result. The average-phase approximation of the metron computation was replaced here by a more accurate Monte Carlo computation for an ensemble of 10,000 particles, in which the phase of the primary wave of each particle was computed separately as a function of the point y_0 at which the particle passes through one of the slits and

---

[1]Figures in colour will be available only in electronic version.

the particle path, given the initial path values θ_0, v_0. The values y_0 were distributed uniformly over the two slits, while the (statistically independent) distributions of the initial values θ_0, v_0 were taken as Gaussian (see Fig. 1). Other adjusted model parameters were the magnitude and rate of decrease of the modulation function f_r with distance behind the slit. A finite spectral broadening of the incident particle flux was assumed with respect to both magnitude and direction of the particle velocities, as in the refraction experiments of Zeilinger *et al* [13] and Tschernitz *et al* [10] using low-energy neutrons. The authors found good agreement between quantum theory and experiment if in addition to the adjustment of these parameters a suitable background neutron flux was fitted to the data. At the present level of accuracy, however, Fig. 1 suggests that quantum theory cannot be distinguished from the metron model.

Since the quantum theoretical and metron computation of the diffracted particle fluxes in neutron diffraction experiments exhibit real differences in detail, an experimental distinction between the two models should become feasible, once all parameters that enter in the computations are accurately determined. Further careful experiments on the diffraction of neutrons under different conditions, together with more detailed computations of the relevant metron parameters (based on a complete representation of the metron solutions, which is presently lacking), should ultimately lead to a clarification of which of the two models provides a more accurate description of particle interference phenomena.

3 Numerical computation of metron solutions: preliminary results

Metron theory hypothesizes that particles represent bound-state solutions of the Einstein vacuum equations

$$E_{LM} = 0, \tag{3}$$

where E_{LM} is the Einstein tensor in a higher- (we assume 8-) dimensional space $(L, M = 1, \ldots, 8)$ characterized by a background Minkowski metric $\eta_{LM} = \mathrm{diag}\,(1, 1, 1, -1, 1, 1, 1, 1)$. We seek to construct a solution as a perturbation series

$$g_{LM} = \eta_{LM} + \sum_p g_{LM}^{(p)}, \tag{4}$$

with metric perturbations $g_{LM}^{(p)}$ that are periodic with respect to time and the extra-space coordinates and isotropic with respect to three-dimensional physical space,

$$h_{LM}^{(p)} = f^{(p)}(r) P_{LM}^{(p)} \exp i \left(k_A^{(p)} x^A \right), \tag{5}$$

where

$$h_{LM}^{(p)} := g_{LM}^{(p)} - \frac{1}{2} \eta_{LM} \left(\eta^{NO} g_{NO}^{(p)} \right) \tag{6}$$

is the trace-reversed perturbation, $r = (x^i x_i)^{1/2}$ $(i = 1, 2, 3)$, $P_{LM}^{(p)}$ is a constant polarization matrix and the wave-numbers $k_4^{(p)}$ (frequency), and $k_A^{(p)}$, $A = 5, \ldots, 8$ (extra-space wave-numbers) denote the fundamental and higher-harmonic components with respect to a small number (in our application, two, in general, maximally five) base wavenumbers (where "higher harmonic" includes the zero wave-number, $k_A = 0$, associated with the wave-guide).

Substitution of the perturbation expansion into the Einstein equations yields a set of coupled field equations of the general form

$$\left(\partial^N \partial_N + e_n \right) \phi_n = \left\{ \frac{d^2}{dr^2} + 2\frac{d}{dr} - \hat{\omega}^2 + e_n \right\} \phi_n = q_n, \tag{7}$$
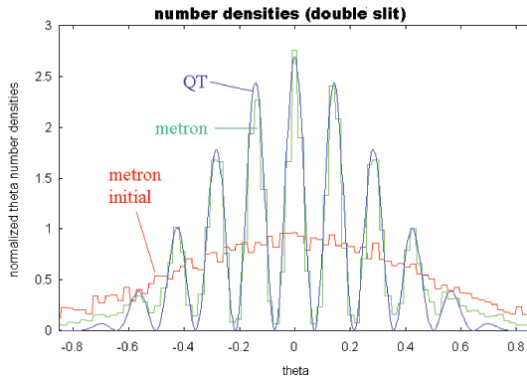
Figure 1. Number densities of refracted parti-cles computed for quantum theory and metron model. Also shown is the assumed near-slit distribution for the metron case.
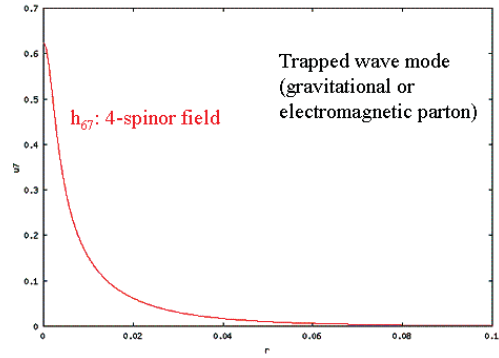
Figure 2. Trapped mode component h_{67} (representing a 4-spinor field) for the gravitational constituent ($k_4 = 999, 55$, $k_5 = 1000$, $\hat{\omega} = 30$). The associated wave-guide components are shown in Fig. 3. A similar form is found for the electromagnetic constituent, ($k_4 = 0$, $k_5 = 30$, $\hat{\omega} = 30$), which yields the wave-guide components shown in Fig. 4.

where ϕ_n denotes the radial function $f^{(p)}(r)$ of a given constituent $h_{LM}^{(p)}$, $\hat{\omega}^2 = k_A k^A$, and the eigenvalue operator e_n and forcing term q_n are nonlinear functions of the set of all constituents. The index n distinguishes between first-harmonic ($n = 1$), higher-harmonic ($n > 1$) and wave-guide ($n = 0$) components. In addition, the fields must satisfy appropriate divergence gauge conditions.

For the lowest (cubic) interaction order, the equations for the first-harmonic constituents ($n = 1$) reduce to a quasi-linear eigenvalue problem, with $q_1 = 0$, where the operator e_1 is quadratic in the first-harmonic constituents and linear in the zero- and second-harmonic constituents. The corresponding equations for the wave-guide ($n = 0$) and forced waves ($n = 2$) are characterized by zero eigenvalue operators ($e_n = 0$) and non-zero source functions q_n that depend quadratically on the first-harmonic fields.

The challenge is to find stationary, bound-state solutions of the complete set of equations. To search for such bound-state solutions of the Einstein vacuum equations in eight-dimensional space, a three-layered system of programs was developed. The first program layer translates the Einstein tensor equations into a set of 52 coupled differential equations for the different trapped-mode, wave-guide and forced-wave constituents associated with the different wave-number base vectors. A valuable check on the algebra of the program was the divergence condition $E_{L,M}^{M} = 0$, valid for any metric field. The second program layer computes the coupling coefficients for the set of differential equations. The third layer, finally, searches for solutions of the non-linear eigenvalue problem, using various iteration methods.

In accordance with the wave-number properties and polarization relations deduced from the inverse modelling analysis of [6, Parts 3 and 4], the electron is characterized by two wave-number vectors lying in the x^4, x^5 plane, while the first-harmonic constituents, corresponding to 4-spinors, were represented by a non-diagonal polarization matrix component P_{67} in the adjacent extra space. The search for bound-state solutions confirmed that this choice was consistent: nonlinear interactions with the zero- and second-order harmonic fields generated no other first-harmonic constituents of different polarization structure.

To obtain periodic far-fields that fall off approximately as r^{-1} rather than exponentially, as required for a de Broglie far field that generates interference effects over large distances, the wave-number components of one of the first-harmonic constituents must be approximately equal: $k_4 \approx k_5$ (so that $\hat{\omega}^2 \approx 0$ in (7)). We refer to this constituent as the gravitational
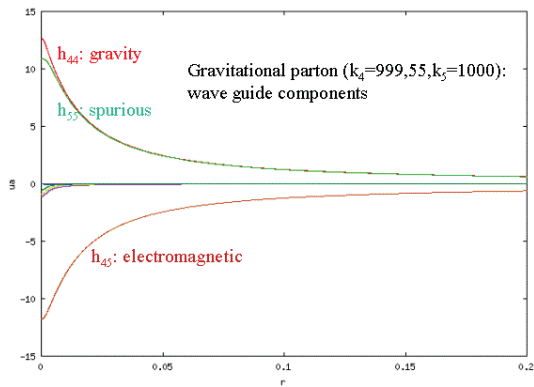
Figure 3. Wave-guide components generated by the gravitational trapped mode shown in Fig. 2. The gravitational (h_{44}), electromagnetic (h_{45}) and spurious extra-space (h_{55}) fields are approximately equal in magnitude.
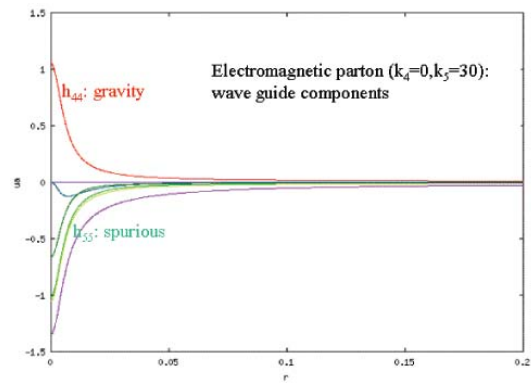
Figure 4. Wave-guide components generated by the electromagnetic trapped mode. There is no electromagnetic field $(h_{45} = 0)$, while the gravitational (h_{44}) and spurious extra-space (h_{55}) fields are of comparable magnitude. The remaining extra-space fields do not exert forces on the particles for $k_6, k_7, k_8 = 0$.

fermionic mode. However, since the strength of the forces experienced by a metron particle is proportional to the wave-number components (k_4, corresponding to mass and gravitational coupling, and k_5, corresponding to charge and electromagnetic coupling, cf. [6, Part 2]), the great disparity ($\sim 10^{-39}$) between the strengths of the gravitational and electromagnetic forces requires that for the second first-harmonic constituent, the wave-number components must then satisfy the inequality $k_4 \ll k_5$. We set $k_4 = 0$, and refer to this constituent as the electromagnetic fermionic mode.

As preparation for the computation of the fully coupled system, we computed first the coupling between the first-harmonic fields and their associated zero-harmonic wave-guide and second-harmonic forced-wave fields separately for the gravitational and electromagnetic fermionic modes (Figs. 2–4). Quasi-bound states were computed through an iterative adjustment procedure analogous to that described in [6, Part 1].

Fig. 2 shows the resulting trapped-mode field for the gravitational fermionic mode; the electromagnetic fermionic mode (not shown) has a similar form. The gravitational first-harmonic field (with assumed wave-number vector components $k_4 = 999,55$, $k_5 = 1000$, yielding $\hat{\omega}^2 = k_5^2 - k_4^2 = 30^2$) generates gravitational (h_{44}) and electromagnetic (h_{45}) far fields, as well as a spurious extra-space (h_{55}) far field, all of nearly the same magnitude (Fig. 3). The corresponding zero-harmonic wave-guide components generated by the electromagnetic fermionic mode (with $k_4 = 0$, $k_5 = 30$, chosen to yield the same exponential fall off, $\hat{\omega} = 30$, as the gravitational mode) are shown in Fig. 4. The electromagnetic far-field is zero in this case. We denote nevertheless the first-harmonic fermionic mode that produces the far fields as the electromagnetic fermionic mode, as it carries the charge wave-number component k_5 that generates the electromagnetic forces (see [6, Part 2]). The second-harmonic fields (not shown) have similar structures and magnitudes as the zero-harmonics, but decrease exponentially rather than as r^{-1} for large r. The fields shown represent only quasi-converged bound states: to achieve convergence of our numerical iteration scheme, the r-scales of the first-harmonic fermionic fields needed to be adjusted by about 10–20 % relative to the scales of the forced zero- and second-harmonic fields.

The question of convergence is not critical, however, at this level of analysis, as it needs to be addressed again for the next step: the construction of a realistic model of the electron by combining the gravitational and electromagnetic fermionic modes and the sets of far fields and second-harmonic fields that they generate into a single model, including the cross-coupling between the two systems. For a realistic electron model, the coupled system must reproduce

the 10^{-39} disparity in the magnitudes of the gravitational and electromagnetic forces (requiring very small ratios of the amplitude and/or wave-number components $k_4 \approx k_5$ of the gravitational fermionic mode relative to the amplitude and/or wave-number component k_5 of the electromagnetic fermionic mode) and at the same cancel the spurious h_{55} wave-guide far field, which would otherwise create an additional (non-observed) force by coupling into the charge k_5. (This problem was encountered already by Kaluza [8] in his original five-dimensional generalization of Einstein's equations, considered later also by Klein [9] and revived fifty years later in general higher-dimensional gravity theory.)

The determination of bound-state solutions for the coupled problem of two fermionic modes requires more sophisticated iteration methods, still in development, than applied above. However, preliminary numerical experiments indicate that solutions with the required properties appear feasible; indeed, an amplitude of the gravitational fermionic mode that is considerably smaller than obtained in the analysis of the individual systems (cf. Fig. 3) is a prerequisite for generating a strongly reduced spurious h_{55} wave-guide field by this component, that is then able to cancel the corresponding spurious h_{55} field generated by the electromagnetic fermionic mode, cf. Figs. 3 and 4 (this is also necessary to justify a perturbation approach for the wave-guide fields generated by the gravitational fermionic mode). It is hoped that the validity of the general metron concept explored in this paper, or possibly the need for revisions (for example, by extension to higher dimensions, or the inclusion of higher order terms in the perturbation expansion) can soon be decided.

4   Outlook

The demonstration that the metron model is able to reproduce the properties of the simplest elementary particle, the electron, is clearly an essential first step in the development of the theory. Assuming that this can be achieved, one then faces the challenge of translating the qualitative results listed in the introduction above into quantitative analysis, using forward rather than inverse modelling methods. However, the task is perhaps not so daunting as it appears at first sight. The program codes developed for the analysis of the two-fermion-component electron system are designed to be applicable also for the five-fermion-component system required to reproduce the particle spectrum of the Standard Model, including gravitational, elecro-weak and strong interactions.

Furthermore, all fields that arise in standard quantum field theory, as well as in quantum theory and classical gravity, appear also in the metron model. The only difference is that the metron model contains also a particle-core region, which acts as the source of the fields, and that the fields represent real physical objects rather than abstract mathematical quantities used to predict the probability outcomes of experiments. However, the nonlinear interactions between the different field constituents are basically the same in both theories, so that most of the computations of quantum theory and quantum field theory can be directly translated into equivalent computations for the metron model.

It has been pointed out by Wolfgang Kundt (private communication) that the presentation of the metron model in terms of higher-dimensional gravity can be replaced by an aesthetically more attractive formulation in standard four-dimensional space-time. This is because all fields in the metron model are assumed to be periodic with respect to the extra-space coordinates, so that the only non-trivial spatial dependence is with respect to four-dimensional space-time. The tensor components of the metric fields in higher-dimensional space can therefore be treated as a fiber bundle dependent only on space-time. The transformation relations of the fibre-bundle fields with respect to coordinate transformations in four-dimensional space-time inferred from higher-dimensional gravity then ensure (for a given set of wave-number vectors) that the extended system of Einstein equations, including all components of the fiber bundle, is invariant

with respect to coordinate transformations in four-dimensional space-time. A reformulation of the metron model using this terminology would be an attractive task.

[1] Bell J.S., On the impossible pilot wave, *Found. Phys.*, 1982, V.12, 989–999.

[2] Bohm D., A suggested interpretation of the quantum theory in terms of "hidden variables", Parts I–III, *Phys. Rev.*, 1952, V.85, 165–179; 180–193.

[3] de Broglie L., L'interprétation de la méchanique ondulataire, *Jorunal de Physique et le Radium*, 1959, V.20, 963–979.

[4] de Broglie L., Non-linear wave mechanics: A causal interpretation, Amsterdam, Elsevier, 1960.

[5] de Broglie L., The current interpretation of wave mechanics: a critical study, Amsterdam, *Elsevier*, 1964.

[6] Hasselmann K., The metron model: elements of a unified deterministic theory of fields and particles, Part 1: The metron concept, *Physics Essays*, 1996, V.9, 311–325; Part 2: The Maxwell–Dirac–Einstein system, *Physics Essays*, 1996, V.9, 460–475; Part 3: Quantum phenomena, *Physics Essays*, 1997, V.10, 64–86; Part 4: The standard model, *Physics Essays*, 1997, V.10, 269–286.

[7] Hasselmann K., The metron model. Towards a unified deterministic theory of fields and particles, in Understanding Physics, Editor A.K. Richter, Copernicus Gesellschaft e.V. Kathlenburg-Lindau, 1998, 154–186.

[8] Kaluza Th., Zum Unitätsproblem der Physik, *Sitzungsber. d. Berl. Akad.*, 1921, 966–972.

[9] Klein O., Quantentheorie und fünfdimensionale Relativitätstheorie, *Z. Phys.*, 1926, V.37, 895–906.

[10] Tschernitz M., Gähler R., Mampe W., Schillinger B. and Zeilinger A., Precision measurements of single slit diffraction with very cold neutrons, *Phys. Lett. A*, 1992, V.164, 365–368.

[11] Wheeler J.A. and Feynman R.P., Interaction with the absorber as the mechanism of radiation, *Rev. Mod. Phys.*, 1945, V.17, 157–181.

[12] Wheeler J.A. and Feynman R.P., Classical electrodynamics in terms of direct particle interaction, *Rev. Mod. Phys.*, 1949, V.21, 425–433.

[13] Zeilinger A., Gähler R., Shull C.G., Treimer W. and Mampe W., Single- and doppel-slit diffraction of neutrons, *Rev. Mod. Phys.*, 1988, V.60, 1067–1073.